Molecular Biology of the Cell
Vol. 5, 1185–1198, November 1994

Metabolic Instability and Constitutive Endocytosis of STE6, the a-Factor Transporter of *Saccharomyces cerevisiae*

Carol Berkower, Diego Loayza, and Susan Michaelis

Department of Cell Biology and Anatomy, The Johns Hopkins University School of Medicine, Baltimore, MD 21205

Submitted May 31, 1994; Accepted September 13, 1994
Monitoring editor: Gerald R. Fink

STE6, a member of the ATP binding cassette (ABC) transporter superfamily, is a membrane protein required for the export of the **a**-factor mating pheromone in *Saccharomyces cerevisiae*. To initiate a study of the intracellular trafficking of STE6, we have examined its half-life and localization. We report here that STE6 is metabolically unstable in a wild-type strain, and that this instability is blocked in a *pep4* mutant, suggesting that degradation of STE6 occurs in the vacuole and is dependent upon vacuolar proteases. In agreement with a model whereby STE6 is routed to the vacuole via endocytosis from the plasma membrane, we show that degradation of STE6 is substantially reduced at nonpermissive temperature in mutants defective in delivery of proteins to the plasma membrane (*sec6*) or in endocytosis (*end3* and *end4*). Whereas STE6 appears to undergo constitutive internalization from the plasma membrane, as do the pheromone receptors STE2 and STE3, we show that two other proteins, the plasma membrane ATPase (PMA1) and the general amino acid permease (GAP1), are significantly more stable than STE6, indicating that rapid turnover in the vacuole is not a fate common to all plasma membrane proteins in yeast. Investigation of STE6 partial molecules (half-and quarter-molecules) indicates that both halves of STE6 contain sufficient information to mediate internalization. Examination of STE6 localization by indirect immunofluorescence indicates that STE6 is found in a punctate, possibly vesicular, intracellular pattern, distinct from the rim-staining pattern characteristic of PMA1. The punctate pattern is consistent with the view that most of the STE6 molecules present in a cell at any given moment could be *en route* either to or from the plasma membrane. In a *pep4* mutant, STE6 is concentrated in the vacuole, providing further evidence that the vacuole is the site of STE6 degradation, while in an *end4* mutant STE6 exhibits rim-staining, indicating that it can accumulate in the plasma membrane when internalization is blocked. Taken together, the results presented here suggest that STE6 first travels to the plasma membrane and subsequently undergoes endocytosis and degradation in the vacuole, with perhaps only a transient residence at the plasma membrane; an alternative model, in which STE6 circumvents the plasma membrane, is also discussed.

INTRODUCTION

The STE6 gene product of *Saccharomyces cerevisiae* is responsible for transporting the **a**-factor mating pheromone out of the cell, thus performing the final step in **a**-factor biogenesis (Michaelis, 1993). STE6 is a 145 kD integral membrane protein, composed of two similar halves; each half contains six predicted membrane spans and a consensus nucleotide binding fold (NBF) domain (Kuchler *et al.*, 1989; McGrath and Varshavsky, 1989; Berkower and Michaelis, 1991). Based on homology and on its predicted structure, STE6 belongs to the ATP binding cassette (ABC) family of proteins, whose members also include the mammalian multidrug resistance protein (MDR), the cystic fibrosis transmembrane conductance regulator (CFTR), transporters associated with

antigen processing (TAPs), and a variety of bacterial periplasmic permeases (Higgins, 1992). Because of its transport function for **a**-factor, STE6 is presumed to lie on the plasma membrane.

Membrane proteins in eukaryotic cells can either reside stably in the membrane or undergo dynamic intracellular movement, including recycling, via the endocytic pathway. Most of what is known about the metabolism of membrane proteins in yeast has been learned by studying the mating pheromone receptors, STE2 and STE3. Upon binding of these receptors to extracellular pheromone, the ligand-receptor complex undergoes endocytosis and is transported to the vacuole (Jenness and Spatrick, 1986; Riezman, 1993). In the vacuole, both the pheromone (as shown for **a**-factor) and its receptor are degraded by vacuolar proteases. In addition to this pheromone-stimulated mode of endocytosis, the receptor is subject to a second mode of endocytosis, which occurs constitutively and is independent of pheromone (Davis *et al.*, 1993). Constitutive endocytosis has been examined by monitoring the metabolic half-lives of the receptors in the absence of pheromone. Mutations in STE3 that block only its constitutive endocytosis have been described (Davis *et al.*, 1993). Cellular components involved in the endocytosis of the pheromones and/or their receptors have also been identified. Two mutants, *end3* and *end4*, were isolated on the basis of their defect in internalization of α-factor and may disrupt an early stage of this process (Raths *et al.*, 1993). Other mutants, *end2* (Chvatchko *et al.*, 1986), *ypt7* (Schimmoller and Riezman, 1993), and *ren1*, which is allelic to *vps2* (Davis *et al.*, 1993), may be defective in later stages of transport of proteins to the vacuole. A *ren1/vps2* mutant is also defective in the sorting of resident vacuolar proteins (Rothman and Stevens, 1986; Robinson *et al.*, 1988; Raymond *et al.*, 1992). Indeed, biochemical analysis indicates that the endocytic (end) and vacuolar protein sorting (vps) pathways intersect in a common pre-vacuolar compartment, as seen in mammalian cells (Vida *et al.*, 1993). Internalization of **a**-factor also requires elements of the actin cytoskeleton (*ACT1*, *SAC6*; [Kubler and Riezman, 1993]), and internalization is retarded by mutations in the clathrin heavy chain (Tan *et al.*, 1993). In addition to STE2 and STE3, the uracil permease (FUR4) has been observed to undergo degradation in a *PEP4*, *END3*, and *END4* dependent manner under conditions of nutrient deprivation (Volland *et al.*, 1994). However, aside from FUR4 and the pheromone receptors, the fates of other plasma membrane proteins in yeast have not been carefully examined.

We are interested in understanding the intracellular trafficking of STE6. Here we have examined the metabolic stability of STE6 by pulse-chase analysis. Our results indicate that STE6 is metabolically unstable and that this instability is *PEP4*-dependent, suggesting that degradation of STE6 is carried out by vacuolar proteases. At nonpermissive temperature, mutants defective in either endocytosis (*end3* and *end4*) or the secretory pathway (*sec6* and *sec1*) fail to degrade STE6 rapidly, presumably because they prevent STE6 from reaching the vacuole. These experiments provide evidence that STE6 is routed to the vacuole via endocytosis from the plasma membrane. By determining the turnover rates of STE6 partial molecules, we find that both halves of STE6 contain sufficient information to mediate internalization, suggesting that, if an endocytosis signal is present, it is likely to be redundant. We have also examined the cellular localization of STE6 by indirect immunofluorescence. In contrast to the cell surface staining pattern we observe for the plasma membrane ATPase, PMA1, STE6 exhibits a punctate staining pattern that may reflect its presence in intracellular vesicles. We suggest that the punctate, potentially vesicular, staining pattern in wild-type cells, coupled with the absence of detectable cell-surface staining, may mean that at any given moment, the majority of STE6 molecules in the cell are either *en route* to or *en route* from the plasma membrane. The rapid turnover and apparently intracellular localization of STE6 raise some interesting questions regarding **a**-factor export.

MATERIALS AND METHODS

Strains, Media, and Growth Conditions

Yeast strains used in this study are listed in Table 1. SM1058 was formerly designated EG123 (Michaelis and Herskowitz, 1988). The *ste6::LEU2* allele in strain SM1563 was generated via one-step gene replacement of the wild-type *STE6* gene in SM1058, with the use of a linear fragment from pSM197 (see below). Transformations were performed either by the lithium acetate method (Ito *et al.*, 1983) or by the method of Elble (1992). In the latter case, 10 μl of 1 M dithiothreitol (DTT) was added to each 500 μl transformation, which resulted in an increase in the efficiency of transformation. SC dropout medium (-Leu or -Ura) was prepared as previously described (Michaelis and Herskowitz, 1988). Experiments were performed at 30°C, except where noted.

Plasmid Constructions

The shuttle vectors used in this study are pRS314 (*CEN6 TRP1*), pRS315 (*CEN6 LEU2*), and pRS316 (*CEN6 URA3*) (Sikorski and Hieter, 1989). The vector pRS315–1 (*CEN6 LEU2*) and the STE6-containing plasmids pSM192 (*CEN6 URA3 STE6*), pSM322 (*CEN6 LEU2 STE6*), pSM435 (2 μm *LEU2 STE6*), pSM415 (*CEN6 LEU2 N-Half*), and pSM434 (*CEN6 TRP1 C-Half*) have been previously described (Berkower and Michaelis, 1991). The plasmid pPL257 (*CEN6 GAP1::FLU1*), provided by Per Ljungdahl and Gerald Fink, contains an HA-tagged version of *GAP1* (Ljungdahl *et al.*, 1992).

To construct a plasmid for generating a chromosomal *ste6::LEU2* allele, the 6 kb *SalI-Hin*dIII *STE6* fragment from pBR322-STE6 (Wilson and Herskowitz, 1984) was inserted into the polylinker of pSM195 (pUC18 lacking a *Bam*HI site), yielding pSM196. A *Sal*I fragment containing the *LEU2* gene (Sikorski and Hieter, 1989) was cloned into the *Sal*I site of pUC18, generating pSM194. pSM196 was digested with *Bam*HI and *Pst*I, and a 1.4 kb portion of *STE6* was replaced with the *Bam*HI-*Pst*I *LEU2* fragment from pSM194, to produce pSM197. Plasmid pSM197 was used to generate the *ste6::LEU2* disruption in strain SM1563 (above).

Table 1. Yeast strains used in this study

Strain	Genotype	Reference or Source
SM1058	*MAT***a** *ura3-52 leu2-3,112 his4 trp1 can1*	This lab
SM1708	SM1058 [p*CEN6 LEU2*]	Transformant of SM1058 with pRS315
SM2178	SM1058 [p2μm *TRP1 PGK-STE6*]	Transformant of SM1058 with pSM198
SM2217	SM1058 [p*CEN6 URA3 GAP1::FLU1*]	Transformant of SM1058 with pPL257
SM1059	*MATα ura3-52 leu2-3,112 his4 trp1 can1*	This lab
SM2180	SM1059 [p2μm *TRP1 PGK-STE6*]	Transformant of SM1059 with pSM198
SM1563	*MAT***a** *ura3-52 leu2-3,112 his4 trp1 can1 Δste6::LEU2*	This study
SM1564	SM1563 [p*CEN6 URA3 STE6*]	Transformant of SM1563 with pSM192
SM1646	*MAT***a** *ura3-52 leu2-3,112 his4 trp1 can1 Δste6::URA3*	Berkower and Michaelis, 1991
SM1700	SM1646 [p*CEN6 LEU2*]	Berkower and Michaelis, 1991
SM1783	SM1646 [p*CEN6 LEU2 STE6*]	Berkower and Michaelis, 1991
SM1805	SM1646 [p2μm *LEU2 STE6*]	Berkower and Michaelis, 1991
SM1840	SM1646 [p*CEN6 TRP1 C-Half*]	Transformant of SM1646 with pSM434
SM2029	SM1646 [p*CEN6 LEU2 N-3/4*][p*CEN6 TRP1 C-1/4*]	Transformant of SM1646 with pSM529 and pSM524
SM2046	SM1646 [p*CEN6 TRP1 N-Half-HA*]	Transformant of SM1646 with pSM537
SM2285	SM1646 [p*CEN6 LEU2 N-1/4-HA*]	Transformant of SM1646 with pSM549
GPY74-15C	*MAT***a** *ura3-52 leu2-3,112 trp1-289 sst1-3 his4* and/or *his6*	G. Payne
SM2083	GPY74-15C [p*CEN6 URA3 STE6*]	Transformant of GPY74-15C with pSM192
SM2473	GPY74-15C [p2μm *URA3 STE6-HA*]	Transformant of GPY74-15C with pSM693
GPY385	*MAT***a** *ura3-52 leu2-3,112 trp1-289 sst1-3 his4* and/or *his6 Δpep4::LEU2*	G. Payne
SM2085	GPY385 [p*CEN6 URA3 STE6*]	Transformant of GPY385 with pSM192
SM2474	GPY385 [p2μm *URA3 STE6-HA*]	Transformant of GPY385 with pSM693
NY13	*MAT***a** *ura3*	P. Novick
SM2478	NY13 [p*CEN6 URA3 STE6*]	Transformant of NY13 with pSM192
NY17	*MAT***a** *ura3 sec6-4*	P. Novick
SM2479	NY17 [p*CEN6 URA3 STE6*]	Transformant of NY17 with pSM192
RH266-1D	*MAT***a** *ura3 leu2 his4 bar1-1 end3^{ts}*	Raths *et al.*, 1993
SM2227	RH266-1D [p*CEN6 LEU2 STE6*]	Transformant of RH266-1D with pSM322
RH268-1C	*MAT***a** *ura3 leu2 his4 bar1-1 end4^{ts}*	Raths *et al.*, 1993
SM2228	RH268-1C [p*CEN6 LEU2 STE6*]	Transformant of RH268-1C with pSM322
SM2559	RH268-1C [p2μm *URA3 STE6-HA*]	Transformant of RH268-1C with pSM693
RH144-3D	*MAT***a** *ura3 leu2 his4 bar1-1*	Raths *et al.*, 1993
SM2229	RH144-3D [p*CEN6 LEU2 STE6*]	Transformant of RH144-3D with pSM322
SM2560	RH144-3D [p2μm *URA3 STE6-HA*]	Transformant of RH144-3D with pSM693

pSM351, which has no *Bam*HI site in either *STE6* or the vector, was the parental plasmid for generating quarter molecules (below). pSM351 was constructed by first introducing a silent codon change (GGA → GGG) into pSM192 at nucleotide 1002 of *STE6* using oligo SM-36 (5′-ATTTCGCTTGGACCCATCTTTTAATA-G3′), which eliminates the native *Bam*HI site, resulting in plasmid pSM413. Subsequently, the 6 kb *Sal*I-*Hind*III *STE6* fragment was subcloned from pSM413 into pRS315–1 to generate pSM351 (*CEN6 LEU2 STE6*).

To epitope tag full-length and partial STE6 molecules, we used a triply iterated epitope (HA) from influenza hemagglutinin, which is recognized by the monoclonal antibody 12CA5, a subclone of H26D08 (Niman *et al.*, 1983; Wilson *et al.*, 1984). This 111 bp epitope tag was provided by G. Tokiwa and B. Futcher as a *Not*I fragment in the vector GTEP1 (Tyers *et al.*, 1992). The *Not*1 ends of this insert were converted to *Bgl*II ends by isolating the *Not*I fragment from GTEP1, blunting the ends with the Klenow fragment of DNA polymerase I, ligating on *Bgl*II linkers and subcloning into the *Bgl*II polylinker site in the pUC derivative pLH1 (Howard and Ortlepp, 1989), generating pSM492. To tag the C-terminus of the N-Half of STE6, the 123 bp HA-containing *Bgl*II fragment from pSM492 was ligated into the *Bam*HI site of pSM526, producing pSM537 (*CEN6, TRP1 N-Half-HA*). This *N-Half-HA* construct retained the ability to complement a *Δste6* strain when co-expressed with *C-Half* of *STE6*.

We also generated an HA-tagged version of full-length STE6 to facilitate visualization of STE6 by indirect immunofluorescence. By using oligonucleotide SM-160 (5′ -CTGTACTAGTTGGGGATCC-AAACCTTGATTGA-3′), a *Bam*HI site was introduced into pSM579 (a pSM531 derivative with a *Hind*III site at -10 of *STE6*) at a position corresponding to residue 68, generating plasmid pSM649. The 123 bp *Bgl*II fragment from pSM492 was inserted into this new *Bam*HI site, resulting in the plasmid pSM650, which encodes an epitope-tagged version of STE6 (*STE6-HA*). Subsequently, the six kb *Sal*I-*Not*I fragment bearing *STE6-HA* was subcloned in several steps into pSM217 (2 μm *URA3*), generating pSM693 (2 μm *URA3 STE6-HA*). pSM693 contains several silent codon changes that generate *Bam*HI sites within *STE6*. In this construct, the HA tag is in a predicted extracellular loop of STE6, between the first and second membrane spans. The *STE6-HA* construct complements a *Δste6* mutant for mating.

For construction of quarter-molecules, we used site-directed mutagenesis to generate *Bam*HI sites at positions corresponding to residues 7, 337, 1019, and 1290 of STE6 in pSM351 (*CEN6 LEU2 STE6*). All sites were inserted in the same reading frame. Pairs of *Bam*HI sites were introduced into the same molecule by producing mutations singly and then combining them in a ligation. Through these manipulations we generated plasmids pSM519 (*CEN6 LEU2 STE6* [*Bam*HI at codons 337 and 1290]) and pSM520 (*CEN6 LEU2 STE6* [*Bam*HI at codons 7 and 1019]). In no case did introduction of a *Bam*HI site cause a loss of STE6 function. Plasmids were cut with *Bam*HI to drop out a portion of *STE6* and then religated to generate the partial molecules pSM521 (*CEN6 LEU2 N-1/4*) and pSM522 (*CEN6 LEU2 C-1/4*), respectively. pSM549 (*CEN6 LEU2 N-1/4-HA*) was made by splicing an *Xba*I frag-

ment containing the N-terminus of *STE6* from pSM539 (*CEN6 LEU2 STE6* with the triple HA tag inserted at residue 7) into the *Xba*I site of *N-1/4* from pSM521. pSM524 (*CEN6 TRP1 C-1/4*) was made by subcloning the *Sal*I-*Sac*II fragment containing *C-1/4* from pSM522 into pRS314. Construction of pSM529 (*CEN6 LEU2 N-3/4*) will be described elsewhere. All partial molecules contain the *STE6* promoter, the N-terminal seven residues of STE6, and the *STE6* transcription termination region.

To generate a plasmid constitutively expressing *STE6*, the *STE6* gene was placed downstream of the phosphoglycerate kinase (*PGK*) promoter in several steps (Chen, 1993). A *STE6-lacZ* plasmid, pSM420 (also known as CY84 or d2 [Wilson and Herskowitz, 1986]), in which most of the 5′ regulatory region of *STE6* is deleted, was used as the starting construct. First, a *Bam*HI-*Eco*RI fragment containing the 5′ portion of *STE6* was subcloned from d2 into pRS316 to yield pPC4. Second, an *Eco*RI-*Hind*III fragment from pSM64 that contains the 3′ portion of *STE6* was subcloned into pPC4 to generate pSM193, which contains a promotorless *STE6* with an intact coding sequence. Third, a filled-in 5.0 kb *Hind*III-*Pvu*I fragment was subcloned from pSM193 into the filled-in *Eco*RI site of YEpIPT [a PGK-driven constitutive expression vector (Hitzeman *et al.*, 1982)], to generate pSM198 (2μm *TRP1 PGK-STE6*).

Metabolic Labeling and Immunoprecipitation of STE6, PMA1, and GAP1

For immunoprecipitation of STE6, cells were grown until saturation in SC dropout medium at 30°C (or at 24–26°C for experiments involving temperature sensitive strains). Cultures were then diluted back 1:20 into the same medium at the same temperature and grown for 1–3 doublings, to OD_{600} 0.4–1.0. For each sample, 2.5 OD_{600} units of cells were resuspended in 0.25 ml fresh medium and preincubated at 25°C, 30°C, or 37°C for 15 min (5 min for *end* mutants and the isogenic wild-type strain). For pulse-chase analysis, cellular proteins were labeled with 100–150 μCi Tran[^{35}S]-label (ICN) for 10 min. The chase was initiated by addition of cold methionine and cysteine to a final concentration of 40 mM each and terminated at various time points by addition of cells to an equal volume of ice-cold 2X azide stop mix (40 mM cysteine, 40 mM methionine, 20 mM NaN_3). Cell lysis by base treatment, trichloroacetic acid (TCA) precipitation of proteins, and immunoprecipitation with STE6 antiserum were performed as described previously (Berkower and Michaelis, 1991, 1993), except that unlabeled Δ*ste6* cells were omitted from the immunoprecipitation. For analysis of N-Half-HA, N-1/4-HA, and GAP-HA fusion proteins, we used the mouse monoclonal antiserum 12CA5 (ascites fluid; Babco, Richmond, CA). Affinity-purified PMA1 antiserum was provided by D. Perlin and C. Slayman. Sodium dodecyl sulfate-polyacrylamide gel electrophoresis (SDS-PAGE) was carried out using 8% acrylamide gels. To evaluate the effects of particular mutations on STE6 turnover, each mutant strain was analyzed together with the isogenic wild-type strain.

For determination of STE6, PMA1, and GAP1 half-lives, gels were analyzed by Phosphorimager (Molecular Dynamics, Sunnyvale CA). STE6, PMA1, or GAP1 counts were quantified in each lane, along with a control band (CTRL) that was present at a constant level over the entire period of chase. For STE6 measurements, the Δ*ste6* strain SM1700 was included in each experiment to provide a background determination ($STE6_{1700}$). The relative amount of STE6 (Y_n) in each lane n was calculated as $Y_n = STE6_n/CTRL_n - STE6_{1700}/CTRL_{1700}$. The percentage of STE6 remaining at each time point was plotted, and a single exponential curve fit was calculated according to the equation $Y = P1 + P2 \times [1 - e^{(-P3 \times X)}] + (P4 \times X)$, using the KFIT software package (Neil C. Millar), where X = time in min, P1 = start point, P2 = amplitude, P3 = rate constant, and P4 = slope. The start point (% STE6 at time 0) was fixed at 100%. The time at which this curve intersected with 50% STE6 remaining was determined to be the half-life of STE6. The optimal curve fit required $P4 \neq 0$, suggesting that the observed rate of STE6 degradation varied between earlier and later time points (this can be seen most clearly for the rates of STE6 degradation in *PEP4* and *END3*, *END4* experiments). Nonetheless, we found that the half-life of STE6 in these strains was not significantly changed by fixing P4 at 0.

Indirect Immunofluorescence

Preparation of cells for immunofluorescence was performed essentially as described in Rose et al. (1990). A saturated culture of cells was diluted 1000-fold into SC-URA medium and grown logarithmically at 30°C overnight. For fixation, 5 OD_{600} units of cells were harvested at 2500 rpm in a Beckman TJ-6 centrifuge (Beckman, Fullerton, CA) and resuspended in 5 ml KP buffer (0.1 M potassium phosphate, pH 6.5), formaldehyde (0.6 ml of 37%) was added, and cells were incubated at 30°C with gentle agitation for 40 min. Fixed cells were washed twice in 5 ml KP buffer and once in 5 ml KPS buffer (0.1 M potassium phosphate, pH 6.5, 1.2 M sorbitol), and resuspended in 1 ml KPS buffer. To remove the cell wall, 10 μl of β-mercaptoethanol and 10 μl of 10 mg/ml zymolyase 100T (ICN) were added, and digestion was carried out at 30°C for 40 min. Spheroplasts were washed once with 5 ml KPS.

Fixed, permeabilized spheroplasts were adsorbed to polylysine-coated multiwell slides for 15 min and incubated in PBST (0.04 M K_2HPO_4, 0.01 M KH_2PO_4, 0.15 M NaCl, 0.1% Tween 20, 10 mg/ml BSA, 0.1% NaN_3) for 15 min. Fifteen microliters of primary antibodies diluted in PBST were added to each well. Cells were simultaneously treated with two different primary antibodies: mouse anti-HA monoclonal antibody 12CA5 (ascites fluid; Babco, Richmond, CA), diluted 1:2000, and affinity purified rabbit anti-PMA1 polyclonal antibody (kindly provided by C. Slayman), diluted 1:50. After overnight incubation with primary antibody, wells were subjected to four washes with PBST, addition of secondary antibody in PBST [15 μl of 1:500 rhodamine-conjugated goat-anti-mouse (Boehringer Mannheim, Indianapolis, IN) and 15 μl of 1:500 FITC-conjugated goat-anti-rabbit (Boehringer Mannheim)] and incubation for 2 h at room temperature. Following four washes of the wells with PBST, cells were stained with DAPI and mounting medium (Rose *et al.*, 1990) was added to each well.

RESULTS

STE6 is Metabolically Unstable

To determine whether STE6 is a stable membrane protein or whether it undergoes turnover, we carried out pulse-chase labeling of cellular proteins and examined the fate of STE6 by immunoprecipitation and SDS-PAGE. As shown in Figure 1, this analysis indicates that STE6 is metabolically unstable. The half-life of STE6 is 37 ± 5 min in cells expressing *STE6* from a *CEN* plasmid and grown in minimal medium at 30°C (Figure 1, A and B, CEN). When cells are grown at 37°C, the half-life of STE6 is reduced to 15 to 19 min (see Figures 3 and 4).

To determine whether the amount of STE6 that is synthesized significantly influences its stability, we compared the half-life of STE6 in strains bearing chromosomal *STE6*, a *CEN STE6* plasmid, or a 2 μm *STE6* plasmid. Expression of STE6 from a *CEN* or 2 μm plasmid results in approximately twofold and sevenfold overproduction, respectively, compared with chromosomal STE6 (Figure 1A). STE6 undergoes degradation in each case. The half-life of chromosomally expressed STE6 (39 min) does not differ significantly from that of *CEN* STE6 (37 min); both are somewhat longer than

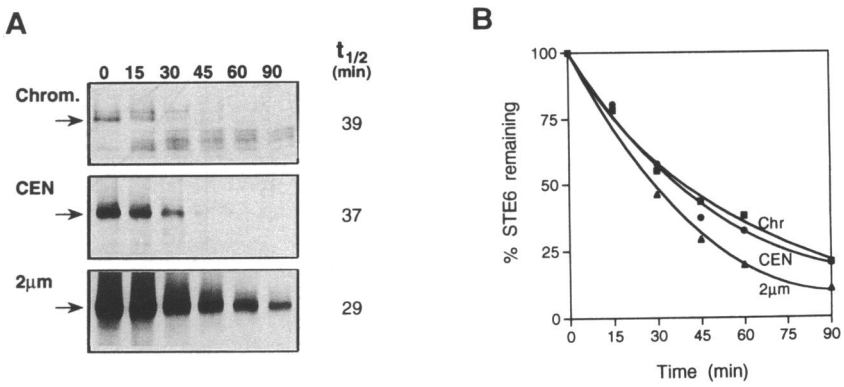

Figure 1. STE6 is metabolically unstable. (A) Pulse-chase analysis of STE6. Strains SM1708, SM1783, and SM1805, which express *STE6* chromosomally or from a *CEN* or 2 μm plasmid, respectively, were pulse-labeled for 10 min and the label was chased for the indicated times (in min). Samples were immunoprecipitated with STE6 antiserum and analyzed by SDS-PAGE and autoradiography. Films were all exposed for 36 h to compare the amounts of STE6 synthesized. The bottom band visible in SM1708 (Chrom.) is not related to STE6, since it is also present in a Δ*ste6* deletion strain. The half-life of STE6 ($t_{1/2}$) is indicated to the right of each gel and was determined as described in MATERIALS AND METHODS. (B) Determination of the half-life of STE6. STE6 counts in each lane were quantified by phosphorimager analysis and graphed as percentage of STE6 remaining vs. time. Values shown are averaged from 3 experiments and have a standard deviation of ~5 min. Determination of curve fits is described in MATERIALS AND METHODS.

that of 2 μm STE6 (29 min). While the rate of STE6 turnover does vary somewhat with its level of expression, more significant is the finding that, regardless of its expression level, STE6 shows a dramatic degree of metabolic instability. For subsequent pulse-chase experiments reported here, we have used strains expressing STE6 from a *CEN* plasmid.

STE6 Instability Is PEP4-dependent

The vacuole is the main site of protein degradation in yeast (Jones, 1991b). If STE6 degradation occurs in the vacuole, then STE6 should be stabilized in a *pep4* mutant, which is deficient in several vacuolar protease functions (Ammerer *et al.*, 1986; Woolford *et al.*, 1986). To examine this possibility, we compared the half-life of STE6 in an isogenic pair of strains containing either a wild-type or deleted *PEP4* gene. In contrast to the instability of STE6 in the wild-type strain, STE6 is stabilized in the Δ*pep4* mutant (half-life > 5 h) (Figure 2). Thus, disappearance of STE6 is dependent upon vacuolar proteases. This dependence of STE6 degradation on *PEP4* suggests that STE6 travels to the vacuole and is degraded there.

We have also observed that STE6 degradation is considerably reduced in a wild-type *PEP4* strain following prolonged logarithmic growth. This observation is consistent with previous findings that the activity of the *PEP4* gene product is low during log-phase growth and increases considerably as cells enter stationary phase (Jones, 1991a). However, *PEP4* is expressed in stationary phase cells, and its activity can persist for several generations following dilution of a stationary phase culture into fresh medium. Therefore, to observe *PEP4*-dependent degradation of STE6, we dilute stationary phase cells into fresh medium and permit them to grow logarithmically for no more than three doublings before pulse-chase labeling.

STE6 Instability is SEC6-dependent

STE6 exports **a**-factor from the cell into the culture fluid and is presumed to carry out this function at the plasma membrane (Kuchler *et al.*, 1993). To determine whether STE6 must reach the plasma membrane prior to its degradation in the vacuole, we examined STE6 instability in a *sec6* mutant strain, which exhibits a temperature-sensitive defect in the fusion of post-Golgi secretory

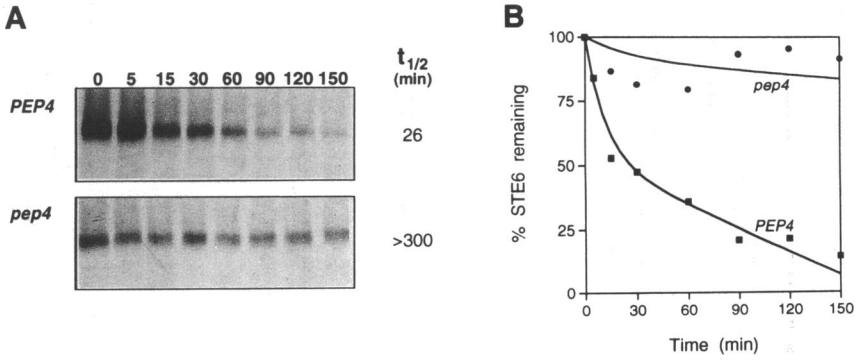

Figure 2. STE6 is stabilized in a *pep4* mutant. (A) Strains SM2083 (*PEP4*) and SM2085 (*pep4*) were pulse-labeled for 10 min and the label was chased for the indicated times (in min). Samples were immunoprecipitated with STE6 antiserum and analyzed by SDS-PAGE. (B) Bands were quantified and graphed as percentage of STE6 remaining vs. time.

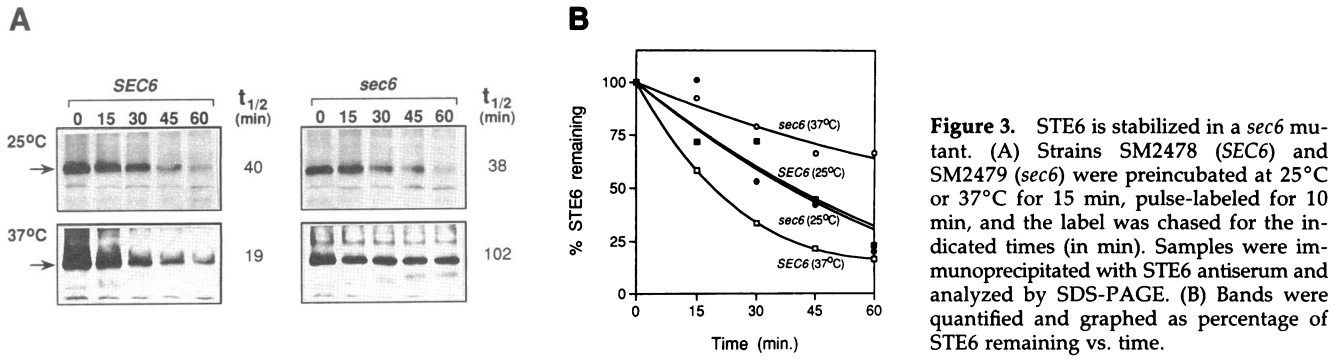

Figure 3. STE6 is stabilized in a *sec6* mutant. (A) Strains SM2478 (*SEC6*) and SM2479 (*sec6*) were preincubated at 25°C or 37°C for 15 min, pulse-labeled for 10 min, and the label was chased for the indicated times (in min). Samples were immunoprecipitated with STE6 antiserum and analyzed by SDS-PAGE. (B) Bands were quantified and graphed as percentage of STE6 remaining vs. time.

vesicles with the plasma membrane. At nonpermissive temperature in a *sec6* strain, secreted proteins and plasma membrane proteins, including the plasma membrane ATPase (PMA1), cannot be transported to the cell surface and accumulate intracellularly in secretory vesicles (Novick and Schekman, 1983; Holcomb *et al.*, 1988; Nakamoto *et al.*, 1991).

To determine whether vacuolar degradation of STE6 is blocked in the absence of *SEC6* function, we examined an isogenic pair of wild-type (*SEC6*) and temperature-sensitive (*sec6*) strains (Figure 3). Cells grown at permissive temperature were subjected to pulse-chase labeling at permissive (25°C) or nonpermissive (37°C) temperature, and the half-life of STE6 was determined. At permissive temperature (25°C), STE6 undergoes degradation at nearly equivalent rates in both the *SEC6* wild-type and *sec6* mutant strains. In contrast, at 37°C, STE6 is stabilized in the *sec6* mutant. We also observed stabilization of STE6 in a *sec1* mutant at nonpermissive temperature, which is blocked at the same stage in the secretory pathway as *sec6*. These results suggest that degradation of STE6 in the vacuole requires its prior transit to the plasma membrane.

At 37°C, the rate of STE6 degradation in the wild-type (*SEC6*) strain is significantly enhanced compared with its rate of degradation in the same strain at 25°C; the half-life of STE6 is 19 min at 37°C and 40 min at 25°C (Figure 3). Disappearance of STE2 from the cell surface is also accelerated at high temperature (Jenness and Spatrick, 1986). It should also be noted that at high temperature, when the half-life of STE6 is shortened, STE6 is dramatically overexpressed [compare the amounts of STE6 synthesized at 25°C vs. 37°C in the wild-type *SEC6* strain (Figure 3A, 0 min)]. Whether the apparent increase in synthesis of STE6 at 37°C is a direct result of its heightened instability at that temperature remains to be determined.

STE6 Instability Is Dependent on END3 and END4

The results described above suggest that STE6 is transported to the vacuole by way of the plasma membrane, perhaps via an endocytic mechanism. Until recently, little was known about the endocytic pathway in yeast. However, it has been demonstrated that the pheromone receptors undergo endocytosis when bound to ligand (Chvatchko *et al.*, 1986; Jenness and Spatrick, 1986 Davis *et al.*, 1993) and that the *END3* and *END4* gene products are required for this process (Raths *et al.*, 1993; Riezman, 1993). *END3* and *END4* also appear to be involved in turnover of the uracil permease (Volland *et al.*, 1994).

We have examined the half-life of STE6 in *end3* and *end4* mutants, which are temperature-sensitive for growth and are unable to internalize pheromone at 37°C. At 37°C, we find that STE6 is stabilized in the

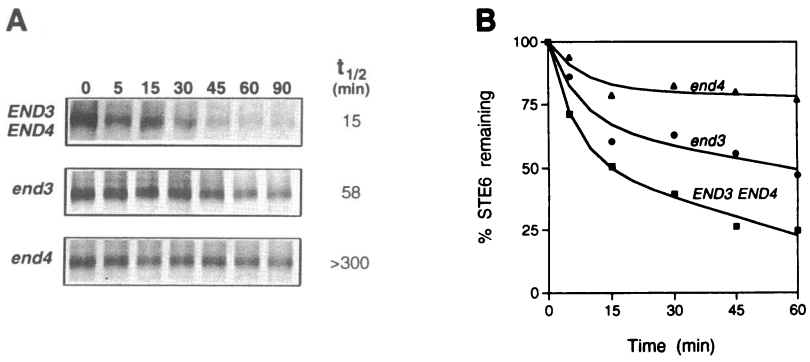

Figure 4. STE6 is stabilized in *end3* and *end4* mutants. (A) Strains SM2229 (*END3 END4*), SM2227 (*end3*), and SM2228 (*end4*) were preincubated at 37°C for 5 min before being subjected to pulse-labeling for 10 min, after which the label was chased for the indicated times (in min). Samples were immunoprecipitated with STE6 antiserum and analyzed by SDS-PAGE. (B) Bands were quantified and graphed as percentage of STE6 remaining vs. time.

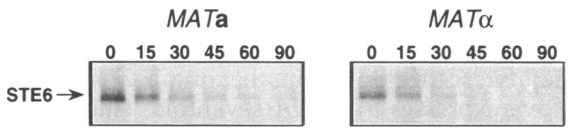

Figure 5. STE6 instability is not affected by mating type. Strains SM2178 (*MAT***a**) and SM2180 (*MATα*) were pulse-labeled for 10 min, and the label was chased for the indicated times (in min). Samples were immunoprecipitated with STE6 antiserum and analyzed by SDS-PAGE.

end3 and *end4* mutants relative to the wild-type strain. The half-life of STE6 is 15, 58, and >300 min in wild-type, *end3* and *end4* strains, respectively (Figure 4). STE6 is stabilized to a greater extent in the *end4* strain than in the *end3* mutant. Similar relative effects of these two *end* mutants were observed for stabilization of the uracil permease, FUR4 (Volland *et al.*, 1994). Since mutations in *END3* and *END4* stabilize STE6, we can conclude that these gene products, which are known to be involved in regulated uptake of pheromone, are also required for constitutive transport of STE6 to the vacuole.

STE6 Half-Life Is Not Affected by Mating Type or Pheromone Induction

STE6 is normally expressed only in *MAT***a** cells and not in *MATα* cells. Thus, the metabolic instability of STE6 might be determined by factors specific to the *MAT***a** mating type. To examine this possibility, we compared the half-life of STE6 expressed from the constitutive *PGK* promoter in *MAT***a** and *MATα* cells. By pulse-chase labeling, immunoprecipitation, and SDS-PAGE, we found that STE6 is degraded with identical kinetics in the two cell types (Figure 5). Thus, the instability of STE6 is not dependent on *MAT***a**-specific cellular functions.

After stimulation of *MAT***a** cells with α-factor, STE6 production is increased (Wilson and Herskowitz, 1986; Kuchler *et al.*, 1993) and cells undergo a variety of pheromone-induced changes, including growth arrest and alterations in the synthesis and localization of several mating-related proteins (Sprague and Thorner, 1992). We measured the half-life of STE6 following α-factor treatment, to determine whether pheromone-induced changes were accompanied by a change in STE6 protein stability. We found that STE6 is degraded at identical rates in α-factor induced and uninduced cells. Thus, α-factor treatment does not affect the turnover rate of STE6.

STE6 Partial Molecules Are Unstable

If STE6 contains a unique signal that targets it for internalization and transport to the vacuole, such a signal might be identified by examining partial deletions in which a portion of STE6 is missing. We examined the degradation rates of STE6 "half-molecules", designated N-Half (residues 1–694) and C-Half (residues 695–1080); we have shown previously that co-expression of these two separately encoded halves of STE6 results in transport of **a**-factor, although neither half can function alone (Berkower and Michaelis, 1991, 1993). For the present experiment, we expressed the half-molecules separately to preclude any effects due to their association and determined the rates of N-Half and C-Half degradation by pulse-chase analysis. Our results indicate that when expressed independently, both halves are degraded at the same rate as the full-length protein (Figure 6, A and B). Therefore, if a degradation signal exists, it must be redundantly present in both halves of STE6.

We further subdivided STE6 into N-terminal and C-terminal quarter-molecules (N-1/4-HA and C-1/4) and examined the half-lives of these quarter-molecules (Figure 6, C and D). N-1/4-HA is unstable, and its degradation rate is similar to that of full-length STE6 (Figure 6C). Therefore, the N-terminal portion of STE6 containing the first six membrane spans appears to contain sufficient information to target the molecule for internalization. Degradation of N-1/4-HA is likely to reflect its endocytosis, rather than its localization to the vacuole

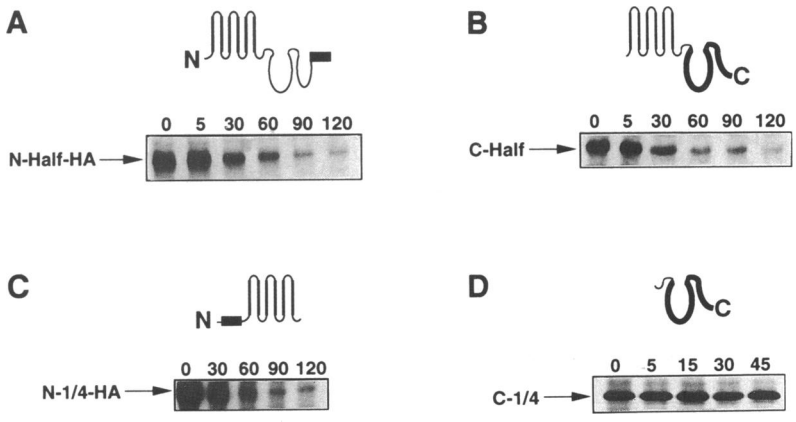

Figure 6. Determination of the stability and function of STE6 partial molecules by pulse-chase analysis. Strains (A) SM2046 (*N-Half-HA*), (B) SM1840 (*C-Half*), (C) SM2285 (*N-1/4-HA*), and (D) SM2063 (*C-1/4*) were pulse-labeled for 10 min and the label was chased for the indicated times (in min). Samples in (A) and (C) were immunoprecipitated with 12CA5 antiserum, which recognizes the HA epitope tag. Samples in (B) and (D) were immunoprecipitated with STE6 antiserum. Immunoprecipitates were analyzed by SDS-PAGE. Each partial molecule is shown schematically. Regions recognized by the antibody used for immunoprecipitation are shown as thick lines or rectangles; the latter represent the HA epitope tag.

by some other pathway, since N-1/4-HA is considerably stabilized in a *sec6* mutant at 37°C. In contrast to N-1/4-HA, C-1/4 does not undergo any apparent degradation in a wild-type strain (Figure 6D). The C-1/4 partial molecule does not associate with the membrane (Berkower and Michaelis, unpublished observation), and this failure to reach the membrane most likely accounts for its lack of endocytosis and degradation.

Other Yeast Plasma Membrane Proteins Are Metabolically Stable Relative to STE6

We considered the possibility that the turnover we observe for STE6 might reflect a general process of membrane recycling in yeast. Were this the case, a short half-life might be a common feature of all yeast plasma membrane proteins. To examine this issue, we analyzed two other yeast plasma membrane proteins, the plasma membrane ATPase, PMA1, and the general amino acid permease, GAP1. Our results indicate that, relative to STE6, PMA1 and GAP1 are metabolically stable, with half-lives exceeding 5 h and 2 h, respectively (Figure 7). Our finding that PMA1 is stable is consistent with a previous determination that PMA1 activity disappears with a half-time of 11 h (Benito *et al.*, 1991). The results shown here with GAP1 and PMA1 indicate that rapid turnover is not a universal feature of all plasma membrane proteins. Thus, STE6, STE2, and STE3 comprise a set of proteins that are rapidly turned over, in contrast to at least several other plasma membrane proteins.

STE6 Accumulates in the Vacuole in a Δpep4 Strain

In the experiments presented up to this point, degradation has served as an indirect indicator that STE6 reaches the vacuole. As an independent means to directly assess delivery of STE6 to the vacuole, we have examined the cellular distribution of STE6 by indirect immunofluorescence. To facilitate this analysis, STE6 was tagged with a triply-iterated version of the influenza virus hemagglutinin epitope, HA1 (Tyers *et al.*, 1992). This epitope-tagged version of STE6, designated STE6-HA, complements a Δ*ste6* deletion and its half-life is the same as that of wild-type STE6. We carried out immunofluorescence on strains bearing a 2 μm plasmid that overexpresses *STE6-HA* sevenfold, since staining could not be detected when *STE6-HA* was expressed from a *CEN* plasmid.

We compared the intracellular distribution of STE6-HA in wild-type (*PEP4*) and mutant (Δ*pep4*) cells, using a mouse monoclonal antibody that recognizes the HA epitope (Niman *et al.*, 1983). As a control, the distribution of plasma membrane ATPase, PMA1, was examined in the same cells. In wild-type (*PEP4*) cells, PMA1 shows a rim-staining pattern typical for a plasma membrane protein (Figure 8F). In contrast, STE6 exhibits a punctate staining pattern, which appears to represent intracellular vesicles containing STE6 (Figure 8E). The punctate appearance of STE6 is quite distinct from the rim-staining observed for PMA1. An analogous punctate staining pattern for STE6 tagged with the c-myc epitope has been reported by others (Kuchler *et al.*, 1993); however, these authors interpreted this pattern as plasma membrane staining.

In contrast to its appearance in wild-type cells, STE6-HA does not produce a punctate fluorescence signal in the Δ*pep4* mutant (Figure 8H). Instead, STE6 staining occurs in a vacuolar or perivacuolar pattern, the vacuole being defined by the intracellular "craters" observed by Nomarski microscopy (Figure 8G). STE6 accumulation in the vacuole of the *pep4* mutant provides further evidence that STE6 is transported to the vacuole. In contrast, the PMA1 rim-staining pattern is identical in both *PEP4* and Δ*pep4* strains (Figure 8, F and I), as might be expected, since pulse-chase analysis (above) indicates that PMA1 is not subject to rapid endocytosis and vacuolar degradation.

STE6 Exhibits Plasma Membrane Staining in an end4 Mutant

If STE6 reaches the vacuole by internalization from the cell surface, rather than by some intracellular route, then

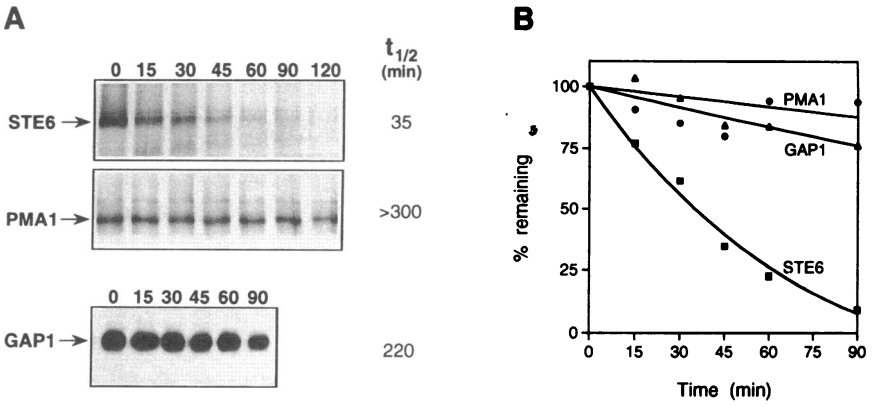

Figure 7. PMA1 and GAP1 are more stable than STE6. (A) Strains SM1783 and SM2217 were pulse-labeled for 10 min and the label was chased for the indicated times (in min). STE6 and PMA1 were immunoprecipitated from SM1783 with STE6 antiserum or affinity-purified PMA1 antiserum, respectively. HA-tagged GAP1 was immunoprecipitated from SM2217 with 12CA5 monoclonal antibodies. (B) Bands were quantified and graphed as percentage of STE6, PMA1, or GAP1::FLU1 remaining vs. time.

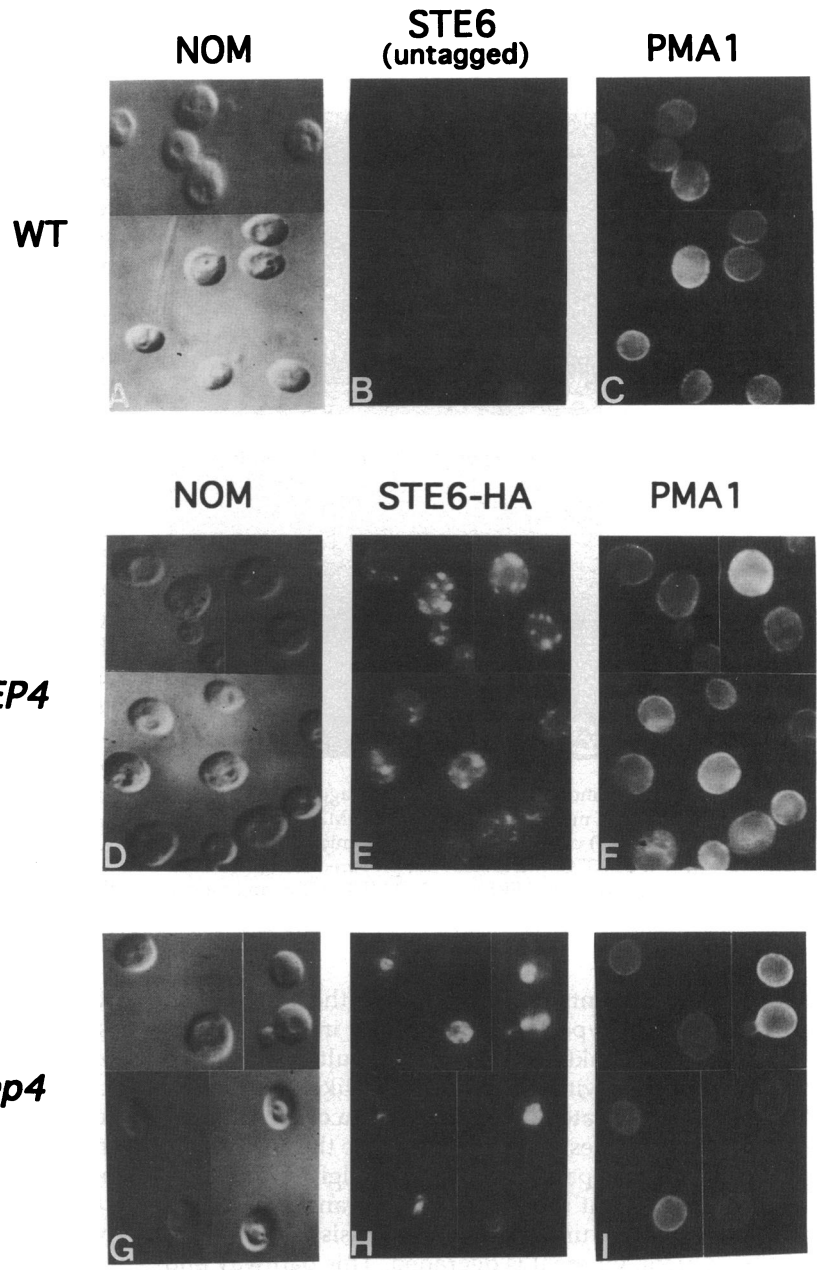

Figure 8. Indirect immunofluorescence of HA-tagged STE6 and PMA1 in wild-type (*PEP4*) and Δ*pep4* cells. Wild-type SM2473 (*PEP4*) and mutant SM2474 (Δ*pep4*) cells, which harbor plasmid pSM693 (*STE6-HA*), were fixed and prepared for immunofluorescence as described in MATERIALS AND METHODS. Cells were stained with antibodies against HA (E,H) and PMA1 (F,I), as described in MATERIALS AND METHODS, and also visualized by Nomarski microscopy (D,G). As a control for background staining of the HA antibody, the strain SM1564 (Δ*ste6* carrying untagged *STE6* on the plasmid pSM192) was processed in parallel (WT; A-C).

we would expect STE6 to accumulate at the plasma membrane in an *end4* mutant. We carried out immunofluorescence of STE6-HA in an isogenic pair of wild-type (*END4*) and mutant (*end4*) strains. In contrast to the punctate staining seen in the *END4* strain, STE6 exhibits a striking rim-staining pattern in the *end4* mutant (Figure 9). This rim-staining pattern is evident even at 25°C, as shown here, presumably reflecting the partial endocytosis defect manifested by *end4* at the permissive temperature. (We have also observed a similar, but fainter, pattern in the *end4* strain at nonpermissive temperature.) Thus, when endocytosis is blocked, STE6 is trapped at the plasma membrane, exposing its normally transient residency at this site. Alternatively, it is formally possible that some indirect effect of the *end4* mutation results in aberrant cell surface localization of STE6.

DISCUSSION

STE6 Undergoes Endocytosis

We have initiated studies to examine the intracellular trafficking of the **a**-factor transporter, STE6. We analyzed the fate of newly synthesized STE6 by pulse-chase

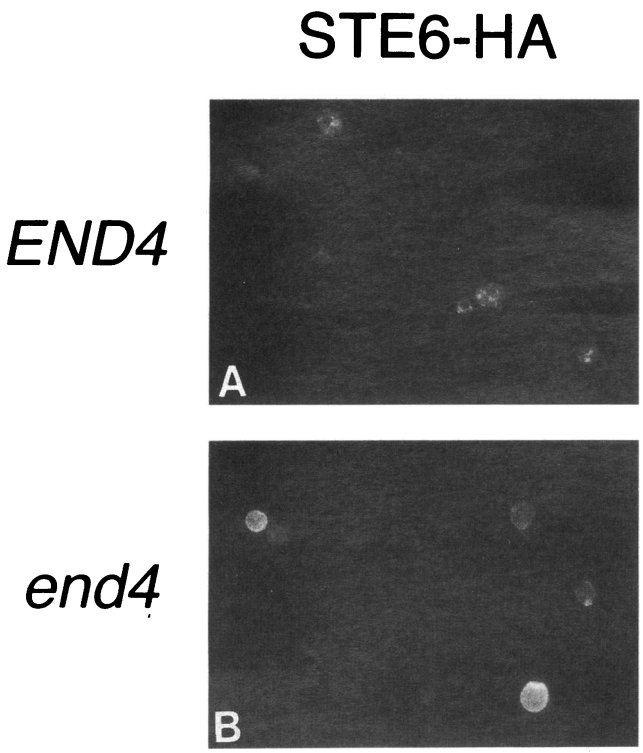

Figure 9. Indirect immunofluorescence of HA-tagged STE6 in wild-type (*END4*) and *end4* mutant cells. Wild-type SM2560 (*END4*) and mutant SM2559 (*end4*) cells, which harbor plasmid pSM693 (*STE6-HA*), were grown at 25°C, then fixed and prepared for immunofluorescence as described in MATERIALS AND METHODS, and stained with antibodies against HA.

labeling experiments and determined the distribution of STE6 in wild-type and *pep4* cells by indirect immunofluorescence. Taken together, our results suggest that STE6 trafficking within the cell most likely occurs by the pathway indicated in Figure 10A. According to this view, newly synthesized STE6 travels to the cell surface via the secretory pathway (ER → Golgi → secretory vesicles), resides at the plasma membrane transiently, and subsequently undergoes endocytosis and delivery to the vacuole, where it is degraded. This pathway and a related but alternative model (shown in Figure 10B) are discussed further below.

The following observations led to the formulation of the STE6 life cycle shown in Figure 10A: 1) pulse-chase metabolic labeling experiments indicate that STE6 is unstable, with a half-life of 30–40 min at 30°C in minimal medium (Figure 1) and an even shorter half-life (15–19 min) at 37°C (Figures 3 and 4); 2) STE6 degradation occurs in the vacuole, as evidenced by the stabilization of STE6 in a *pep4* mutant (Figure 2) and by the vacuolar immunofluorescence staining pattern of STE6 in a *pep4* strain (Figure 8H); 3) STE6 internalization from the plasma membrane appears to occur via endocytosis, since degradation of STE6 is significantly reduced at nonpermissive temperature in the endocytosis-defective mutants *end3* and *end4* (Figure 4), and since STE6 is visible at the cell surface in the *end4* mutant (Figure 9); and 4) in support of the view that STE6 must reach the plasma membrane to undergo endocytosis, STE6 degradation is severely reduced at nonpermissive temperature in the mutant strains *sec6* (Figure 3) and *sec1*, in which delivery of proteins to the plasma membrane is blocked.

In this series of experiments, disappearance of the STE6 protein serves as a marker signifying arrival of STE6 in the vacuole. STE6 could use one of two pathways known in *S. cerevisiae* by which proteins travel to the vacuole; both utilize a common endosomal intermediate (Riezman, 1993; Vida *et al.*, 1993; Nothwehr and Stevens, 1994). One of these pathways, endocytosis, involves internalization of proteins from the plasma membrane to an endosome, and then to the vacuole (Riezman, 1993). The second pathway, the vacuolar protein sorting (vps) pathway, is used for targeting of resident vacuolar proteins, and involves trafficking of these proteins from the Golgi directly to an endosome, and then to the vacuole (Robinson *et al.*, 1988; Raymond *et al.*, 1992; Vida *et al.*, 1993). The vps pathway does not involve the plasma membrane, and is thus independent of post-Golgi secretory functions such as *SEC1* and *SEC6* (Stevens *et al.*, 1982). Because we found that STE6 degradation is dependent on gene products that mediate protein trafficking to and from the plasma membrane (*SEC1*, *SEC6*, *END3*, and *END4*), arrival of STE6 at the plasma membrane appears to be a prerequisite for its metabolic turnover.

However, direct evidence that STE6 is normally associated with the plasma membrane in wild-type cells is lacking (see below). Indeed, because the precise role of the *END4* gene product has not yet been established, it is conceivable that the rim-staining pattern we observe for STE6 in the *end4* mutant is not due to a direct block in internalization of STE6 from the plasma membrane but rather to some indirect "off-pathway" effect of the *end4* mutation. Thus, we cannot completely rule out the possibility that under normal conditions STE6 never reaches the plasma membrane, but instead is routed to the vacuole via a novel intracellular vesicle (as shown in the alternative model, Figure 10B). In accordance with our data, transport of STE6 to and from this novel compartment would of necessity require *SEC1*, *SEC6*, *END3*, and *END4* (although presently, no evidence exists for such a role for these gene products). It is also possible that the hypothetical compartment denoted with a question mark in Figure 10B could recycle STE6 to and from the plasma membrane.

Distinct Fates for Different Membrane Proteins in Yeast

The number of plasma membrane proteins known to undergo endocytosis in *S. cerevisiae* is small, partly be-

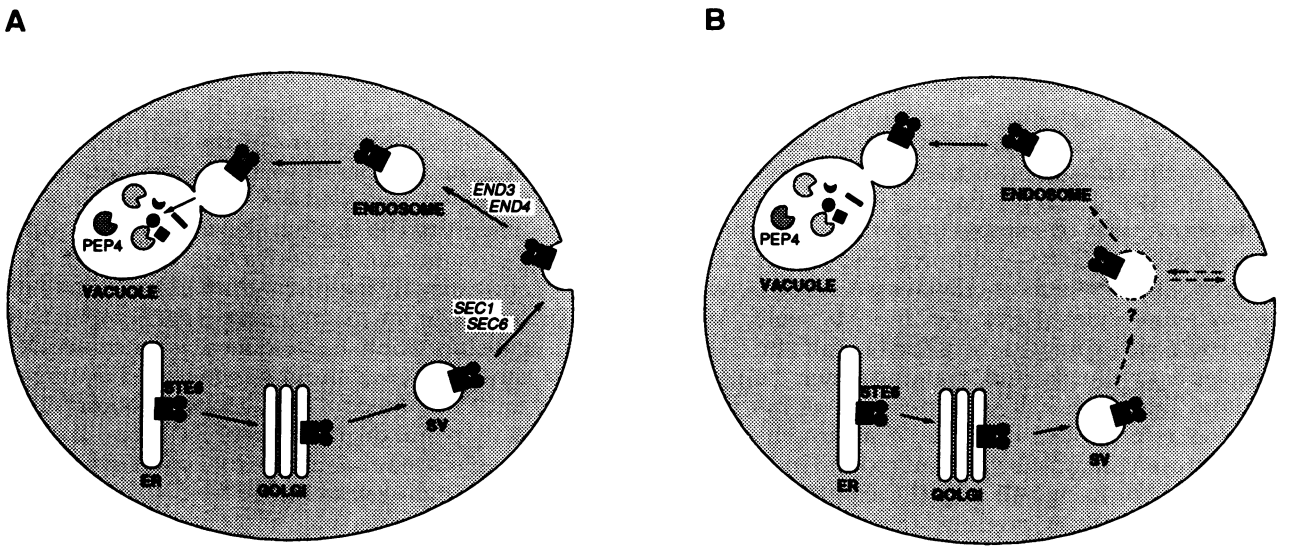

Figure 10. Possible routes for STE6 intracellular trafficking. Two models for the intracellular trafficking of STE6 are shown. STE6 is depicted in the membrane with two domains containing membrane spans (■) and two nucleotide binding domains (●). In the model shown in (A), STE6 travels to the plasma membrane via the ER, Golgi, and post-Golgi secretory vesicles (SV). From the plasma membrane, STE6 undergoes endocytosis into an endosome, which is delivered to the vacuole. In the vacuole, STE6 is degraded by proteases (pacmen) activated by PEP4. The products of the *SEC1*, *SEC6*, *END3*, and *END4* genes act at the indicated steps. (B) STE6 is shown traveling from its point of synthesis to the vacuole, but circumventing the plasma membrane. A hypothetical compartment (designated by a question mark) is shown, which might allow STE6 to circumvent the plasma membrane in its progression to the vacuole. This compartment could cycle to the plasma membrane, releasing its contents into the external medium and thus enabling **a**-factor to exit the cell. Steps of the pathway that are strictly hypothetical are shown as dotted lines.

cause the metabolic fate of most membrane proteins has not been examined experimentally. The best characterized plasma membrane proteins in yeast are the α-factor and **a**-factor pheromone receptors, STE2 and STE3 (Jenness and Spatrick, 1986; Davis *et al.*, 1993; Rohrer *et al.*, 1993; Tan *et al.*, 1993). Studies monitoring the metabolic fates of STE2, STE3, and their pheromone ligands have shown that these receptors are subject to two distinct modes of endocytosis: a ligand (pheromone)-induced mode and a constitutive mode (Davis *et al.*, 1993) (see below). The only other yeast plasma membrane protein demonstrated to undergo endocytic turnover is the *FUR4*-encoded uracil permease. In the case of FUR4, rapid degradation appears to occur only under adverse conditions (Volland *et al.*, 1994). The results presented here indicate that STE6 can be added to the list of membrane proteins that are subject to endocytosis.

Endocytosis of STE6 occurs under normal growth conditions in a constitutive manner. Exogenous treatment of *MAT***a** cells with α-factor does not influence the half-life of STE6. Furthermore, *MAT*α cells that express *STE6* exhibit normal STE6 turnover (Figure 5). The half-life of STE6 (≅37 min at 30°C) does not differ substantially from that reported for the degradation of STE3 via constitutive endocytosis (≅20 min [Davis *et al.*, 1993]), suggesting that internalization of both STE6 and the pheromone receptors may be mediated by a common machinery.

At the outset of these studies there was no *a priori* reason to anticipate that STE6 would undergo rapid metabolic turnover in cells. Our results led us to ask whether constitutive endocytosis might be a feature common to all plasma membrane proteins in yeast, perhaps reflecting a general phenomenon of membrane recycling. To address this issue, we investigated the metabolic fate of two non-mating-related membrane proteins, the plasma membrane ATPase, PMA1 (Serrano, 1991), and the general amino acid permease, GAP1 (Ljungdahl *et al.*, 1992). In contrast to STE6, neither of these plasma membrane proteins exhibits significant metabolic instability (Figure 7 and [Benito *et al.*, 1991]). Thus, we conclude that there exist at least two distinct classes of membrane proteins in yeast: those that undergo rapid endocytosis (STE2, STE3, STE6) and those that do not (PMA1, GAP1). Furthermore, our studies establish STE6 as a potentially useful marker for identifying endocytic vesicles.

Is a Signal Required for Endocytosis of STE6?

The existence of two (or more) distinct classes of proteins with respect to turnover rates leads to the question of whether a specific signal distinguishes these two classes. For instance, proteins destined for endocytosis might contain an "internalization signal", whereas long-lived proteins that remain in the membrane might lack such

a signal. Alternatively, endocytosis of membrane proteins could occur by default, so that long-lived proteins might contain a "retention signal". To begin to address this question, we examined the stability of STE6 partial-molecules. STE6 is comprised of two homologous halves joined by a linker region (Kuchler *et al.*, 1989; McGrath and Varshavsky, 1989; Michaelis, 1993); we have previously shown that co-expression of the two separately encoded halves of STE6 results in transport of **a**-factor, presumably reflecting a functional association between these half-molecules (Berkower and Michaelis, 1991, 1993). Here, we expressed the STE6 N-Half and C-Half molecules individually and examined their half-lives. We found that each half is as unstable as full-length STE6 (Figure 6, A and B). Thus, if an internalization signal is present, it must be present redundantly in both halves of STE6. Each half of STE6 contains a hydrophobic domain with six predicted membrane spans, and a nucleotide binding domain, thought to face the cytosol. We further subdivided STE6 into quarter-molecules and found that the STE6 N-1/4 molecule, which consists mainly of six membrane spans, contains sufficient information to promote its own internalization at a rate comparable to that of full-length STE6 (Figure 6C). As in the case of full-length STE6, the STE6 N-1/4 molecule is stabilized in a *sec6* mutant (Berkower and Michaelis, unpublished observation). In contrast, the STE6 C-1/4 molecule, which contains a nucleotide binding domain and no membrane spans, remains soluble in the cell and is metabolically stable (Figure 6D). Thus, we hypothesize that if STE6 contains an internalization signal, it is likely to lie within the membrane spans of STE6 or the loops that connect them. An internalization signal directing pheromone-induced endocytosis of the α-factor receptor, STE2, resides in the C-terminal region of the receptor (Konopka *et al.*, 1988; Reneke *et al.*, 1988; Rohrer *et al.*, 1993), and the C-terminal region of the **a**-factor receptor, STE3, has been shown to contain information required for its constitutive turnover (Davis *et al.*, 1993). It will be interesting to determine whether STE6 possesses endocytosis signals resembling those in STE2 and STE3.

Possible Roles for Endocytosis and Turnover of STE6

Why might cells synthesize STE6 constitutively, only to degrade it shortly thereafter? Several biological roles for the endocytosis and degradation of STE6 can be considered. First, clearing STE6 from the cell surface via endocytosis could improve the efficiency of mating-type interconversion. While most laboratory strains exist stably as one mating type or the other (*MAT***a** or *MAT*α), yeast strains in the wild are usually homothallic (*HO*$^+$) and are thus capable, in a single generation, of switching their mating-type, via conversion of the *MAT* locus. We have found that when *MAT*α cells are artificially made to express both **a**-factor and STE6, they secrete **a**-factor, activate their endogenous **a**-factor receptors, and respond by arresting growth, which is detrimental to viability (Chen, 1993). Constitutive endocytosis of STE6 ensures its rapid removal from the cell surface, thus minimizing the number of *MAT***a**-specific proteins remaining in newly switched *MAT*α cells. Similar reasoning has been used to explain constitutive endocytosis of the pheromone receptors (Davis *et al.*, 1993).

A second rationale for internalization and degradation of STE6 relates to the mating process itself. Immediately after zygote formation, haploid mating functions are no longer transcribed, and the existing haploid mating machinery must be turned off (Sprague and Thorner, 1992). Internalization and degradation of STE6 and the pheromone receptors may contribute to rapid desensitization of the mating pathway in newly formed zygotes.

Endocytosis may also play a role during the courtship phase of mating (Jackson *et al.*, 1991), when cells shmoo and form mating projections. The cell's secretory apparatus is polarized to the shmoo tip, so that newly synthesized proteins are directed to this site (Baba *et al.*, 1989). Concentration of STE6, hence of **a**-factor transport, at the shmoo tip is likely to increase the local concentration of **a**-factor, affecting partner discrimination. Indeed, others have observed by immunofluorescence that STE6 concentrates at the shmoo tip in MAT**a** cells following α-factor treatment, which could result from a redistribution of resident STE6 molecules to this site (Kuchler *et al.*, 1993). We favor an alternative possibility, namely, that STE6 concentration at the shmoo tip reflects a decrease in STE6 at other cellular sites due to constitutive endocytosis of older STE6 molecules, combined with a pheromone-induced increase in synthesis of new STE6, all of which goes to the shmoo tip. Thus, as has also been hypothesized for the pheromone receptors (Davis *et al.*, 1993), constitutive endocytosis may enhance the emergence of STE6 asymmetry in shmoos.

Finally, a fourth role can be considered for the constitutive endocytosis of STE6, one which could also pertain to non-mating-related proteins. Because STE6 is not essential for cell viability, its constitutive degradation may be used to furnish "raw material" for the synthesis of essential proteins. Such a role may be particularly important during conditions of starvation or stress.

Distribution of STE6 Within the Cell

If STE6 were to reside predominantly on the cell surface, then in wild-type cells it should exhibit a rim-staining pattern by immunofluorescence, similar to the staining pattern observed for the plasma membrane ATPase, PMA1 (Figure 8F). However, we have shown here that STE6 exhibits a punctate staining pattern, suggesting that it resides in intracellular vesicles (Figure 8E). In

addition, our attempts to detect STE6 at the cell surface using external protease treatments (pronase, zymolyase, proteinase K) have yielded negative results, despite our success in using identical procedures to clip PMA1 from the cell's exterior. Thus we conclude that the majority of STE6 molecules in the cell are not normally present at the cell surface.

The apparent lack of STE6 in the plasma membrane seems to conflict with the genetic evidence discussed above, which suggests that STE6 must first be transported to the plasma membrane in a *SEC6*- and *SEC1*-dependent manner to undergo endocytosis. Furthermore, the absence of STE6 from the plasma membrane makes it difficult to understand how STE6 might mediate export of **a**-factor into the culture fluid. These apparent contradictions are reconciled if STE6 is indeed transported to the plasma membrane, but remains there only transiently, so that at any given moment only a small subpopulation of total cellular STE6 is at the cell surface. If the vast majority of STE6 molecules, at any point in time, is *en route* to or from the plasma membrane, then the vesicular staining pattern observed by immunofluorescence could represent STE6 in exocytic or endocytic vesicles; indeed, these vesicles might also represent a recycling compartment between endosomes and the plasma membrane. It has been suggested elsewhere that STE6 may reside in a novel intracellular compartment that fuses with the plasma membrane upon pheromone induction (Kuchler *et al.*, 1993). Clearly, co-localization or co-fractionation of STE6 with proteins whose localization is well-established will be necessary to determine the precise identity of the intracellular compartment(s) detected by STE6 immunofluorescence.

It should also be noted that immunofluorescence was successful only in strains that overexpress STE6 from a 2 μm plasmid; no staining could be observed for strains that express STE6 at a lower level (from a *CEN* plasmid). Similar detection limits have also been reported by others for STE6 (Kuchler *et al.*, 1993). While it is possible that the punctate intracellular staining observed for STE6 could derive solely from its overproduction, which might cause aberrant localization, our findings suggest otherwise. We found that STE6 expressed from a 2 μm plasmid is metabolically unstable, with a degradation rate similar to that of STE6 expressed from a *CEN* plasmid. Thus, many aspects of STE6 trafficking occur normally in these strains, including endocytosis and transport to the vacuole.

Note added in proof. While this manuscript was under review, a study was published by R. Kölling and C.P. Hollenberg (EMBO J. *13*, 3261–3271, 1994) that presents data in substantial agreement with our data on intracellular trafficking and localization of STE6.

ACKNOWLEDGMENTS

We thank Evi Strauss and Eliene Augenbraun for comments on the manuscript; Per Ljungdahl and Gerald Fink for providing an HA-tagged *GAP1* plasmid; Howard Riezman for the *end3* and *end4* mutants; Greg Payne for the *pep4* mutant; Peter Novick for the *sec1* and *sec6* mutants; and David Perlin and Carolyn Slayman for PMA1 antibodies. We thank Eliene Augenbraun for contributing to the construction of HA-tagged *STE6*. This work was supported by a National Institutes of Health grant (GM41223) and a Cystic Fibrosis Foundation grant to S.M. C.B. is a recipient of a predoctoral fellowship from the March of Dimes Foundation, and a predoctoral fellowship from the National Institutes of Health.

REFERENCES

Ammerer, G., Hunter, C.P., Rothman, J.H., Saari, G.C., Valls, V.A., and Stevens, T.H. (1986). *PEP4* gene of *Saccharomyces cerevisiae* encodes proteinase A, a vacuolar enzyme required for processing of vacuolar precursors. Mol. Cell. Biol. *6*, 2490–2499.

Baba, M., Baba, N., Ohsumi, Y., Kanaya, K., and Osumi, M. (1989). Three-dimensional analysis of morphogenesis induced by mating pheromone α factor in *Saccharomyces cerevisiae*. J. Cell Sci. *94*, 207–216.

Benito, B., Moreno, E., and Losario, R. (1991). Half-life of plasma membrane ATPase and its activating system in resting yeast cells. Biochim. Biophys. Acta *1063*, 265–268.

Berkower, C., and Michaelis, S. (1991). Mutational analysis of the yeast **a**-factor transporter STE6, a member of the ATP binding cassette (ABC) protein superfamily. EMBO J. *10*, 3777–3785.

Berkower, C., and Michaelis, S. (1993). Effects of nucleotide binding fold mutations on STE6, a yeast ABC protein. In: Molecular Biology and Function of Carrier Proteins, eds. L. Reuss, J.M. Russell, and M.L. Jennings, New York: The Rockefeller University Press, 130–146.

Chen, P. (1993). Biogenesis of the yeast mating pheromone **a**-factor. PhD Thesis. Johns Hopkins University School of Medicine, Baltimore.

Chvatchko, Y., Howald, I., and Riezman H. (1986). Two yeast mutants defective in endocytosis are defective in pheromone response. Cell *46*, 355–364.

Davis, N.G., Horecka, J.L., and Sprague, G.F., Jr. (1993). *Cis*- and *Trans*-acting functions required for endocytosis of the yeast pheromone receptors. J. Cell Biol. *122*, 53–65.

Elble, R. (1992). A simple and efficient procedure for transformation of yeasts. BioTechniques *13*, 18–20.

Higgins, C.F. (1992). ABC transporters: from microorganisms to man. Annu. Rev. Cell Biol. *8*, 67–113.

Hitzeman, R.A., Hagie, F.E., Hayflick, J.S., Chen, C.Y., Seeburg, P.H., and Derynck, R. (1982). The primary structure of the *Saccharomyces cerevisiae* gene for 3-phosphoglycerate kinase. Nucleic Acids Res. *10*, 7791.

Holcomb, C.L., Hansen, W.J., Etcheverry, T., and Schekman, R. (1988). Secretory vesicles externalize the major plasma membrane ATPase in yeast. J. Cell Biol. *10c*, 641–648.

Howard, L.A., and Ortlepp, S.A. (1989). Construction of cloning/sequencing vectors with an alternative polylinker. BioTechniques *7*, 940–942.

Ito, H., Fukuda, Y., Murata, K., and Kimura, A. (1983). Transformation of intact yeast cells treated with alkali cations. J. Bacteriol. *153*, 163–168.

Jackson, C.L., Konopka, J.B., and Hartwell, L.H. (1991). *S. cerevisiae* α pheromone receptors activate a novel signal transduction pathway for mating partner discrimination. Cell *67*, 389–402.

Jenness, D.D., and Spatrick, P. (1986). Down regulation of the α-factor pheromone receptor in *S. cerevisiae*. Cell *46*, 345–353.

Jones, E.W. (1991a). Tackling the protease problem in *Saccharomyces cerevisiae*. Methods Enzymol. *194*, 428–453.

Jones, E.W. (1991b). Three proteolytic systems in the yeast *Saccharomyces cerevisiae*. J. Biol. Chem. *266*, 7963–7966.

Konopka, J.B., Jenness, D.D., and Hartwell, L.H. (1988). The C-terminus of the *S. cerevisiae* α-pheromone receptor mediates an adaptive response to pheromone. Cell *54*, 609–620.

Kubler, E., and Riezman, H. (1993). Actin and fimbrin are required for the internalization step of endocytosis in yeast. EMBO J. *12*, 2855–2862.

Kuchler, K., Dohlman, H.G., and Thorner, J. (1993). The **a**-factor transporter (*STE6* gene product) and cell polarity in the yeast *Saccharomyces cerevisiae*. J. Cell Biol. *120*, 1203–1215.

Kuchler, K., Sterne, R.E., and Thorner, J. (1989). *Saccharomyces cerevisiae STE6* gene product: a novel pathway for protein export in eukaryotic cells. EMBO J. *8*, 3973–3984.

Ljungdahl, P.O., Gimeno, C.J., Styles, C.A., and Fink, G.R. (1992). SHR3: a novel component of the secretory pathway specifically required for localization of amino acid permeases in yeast. Cell *71*, 463–478.

McGrath, J.P., and Varshavsky, A. (1989). The yeast *STE6* gene encodes a homologue of the mammalian multidrug resistance P-glycoprotein. Nature *340*, 400–404.

Michaelis, S. (1993). STE6, the yeast **a**-factor transporter. Seminars in Cell Biol. *4*, 17–27.

Michaelis, S., and Herskowitz, I. (1988). The **a**-factor pheromone of *Saccharomyces cerevisiae* is essential for mating. Mol. Cell. Biol. *8*, 1309–1318.

Nakamoto, R.K., Rao, R., and Slayman, C.W. (1991). Expression of the yeast plasma membrane [H+]ATPase in secretory vesicles. J. Biol. Chem. *266*, 7940–7949.

Niman, H.L., Houghten, R.A., Walker, L.E., Reisfeld, R.A., Wilson, I.A., Hogle, J.M., and Lerner, R.A. (1983). Generation of protein-reactive antibodies by short peptides is an event of high frequency: implications for the structural basis of immune recognition. Proc. Natl. Acad. Sci. USA *80*, 4949–4953.

Nothwehr, S.F., and Stevens, T.H. (1994). Sorting of membrane proteins in the yeast secretory pathway. J. Biol. Chem. *269*, 10185–10188.

Novick, P., and Schekman, R. (1983). Export of major cell surface proteins is blocked in yeast secretory mutants. J. Cell Biol. *96*, 541–547.

Raths, S., Rohrer, J., Crausaz, F., and Riezman, H. (1993). *end3* and *end4*: two mutants defective in receptor-mediated and fluid-phase endocytosis in *Saccharomyces cerevisiae*. J. Cell Biol. *120*, 55–65.

Raymond, C.K., Howald-Stevenson, I., Vater, C.A., and Stevens, T.H. (1992). Morphological classification of the yeast vacuolar protein sorting mutants: evidence for a prevacuolar compartment in class E *vps* mutants. Mol. Biol. Cell *3*, 1389–1402.

Reneke, J.E., Blumer, K.J., Courchesne, W.E., and Thorner, J. (1988). The carboxy-terminal segment of the yeast α-factor receptor is a regulatory domain. Cell *55*, 221–234.

Riezman, H. (1993). Yeast endocytosis. Trends Cell Biol. *3*, 273–277.

Robinson, J.S., Klionsky, D.J., Banta, L.M., and Emr, S.D. (1988). Protein sorting in *Saccharomyces cerevisiae*: isolation of mutants defective in the delivery and processing of multiple vacuolar hydrolases. Mol. Cell. Biol. *8*, 4936–4948.

Rohrer, J., Bénédetti, H., Zanolari, B., and Riezman, H. (1993). Identification of a novel sequence mediating regulated endocytosis of the G protein-coupled α-pheromone receptor in yeast. Mol. Biol. Cell *4*, 511–521.

Rose, M.D., Winston, F., and Hieter, P. (1990). Methods in yeast genetics: a laboratory course manual. Cold Spring Harbor, NY: Cold Spring Harbor Laboratory Press.

Rothman, J.H., and Stevens, T.H. (1986). Protein sorting in yeast: mutants defective in vacuole biogenesis mislocalize vacuolar proteins into the late secretory pathway. Cell *47*, 1041–1051.

Schimmoller, F., and Riezman, H. (1993). Involvement of Ypt7p, a small GTPase, in traffic from late endosome to the vacuole in yeast. J. Cell Sci. *106*, 823–830.

Serrano, R. (1991). Transport across yeast vacuolar and plasma membranes. In: The Molecular Biology of the Yeast *Saccharomyces*, eds. J.R. Broach, J.R. Pringle, and E.W. Jones, Plainview, NY: Cold Spring Harbor Laboratory Press, 523–585.

Sikorski, R.S., and Hieter, P. (1989). A system of shuttle vectors and yeast host strains designed for efficient manipulation of DNA in *Saccharomyces cerevisiae*. Genetics *122*, 19–27.

Sprague, G.F., and Thorner, J. (1992). Pheromone response and signal transduction during the mating process of *Saccharomyces cerevisiae*. In: The Molecular and Cellular Biology of the Yeast *Saccharomyces*, eds. E.W. Jones, J.R. Pringle, and J.R. Broach, Plainview, NY: Cold Spring Harbor Laboratory Press, 657–744.

Stevens, T., Esmon, B., and Schekman, R. (1982). Early stages in the yeast secretory pathway are required for transport of carboxypeptidase Y to the vacuole. Cell *30*, 439–448.

Tan, P.K., Davis, N.G., Sprague, G.F., and Payne, G.S. (1993). Clathrin facilitates the internalization of seven transmembrane segment receptors for mating pheromones in yeast. J. Cell Biol. *123*, 1707–1716.

Tyers, M., Tokiwa, G., Nash, R., and Futcher, B. (1992). The Cln3-Cdc28 kinase complex of *S. cerevisiae* is regulated by proteolysis and phosporylation. EMBO J. *11*, 1773–1784.

Vida, T.A., Huyer, G., and Emr, S.D. (1993). Yeast vacuolar proenzymes are sorted in the late golgi complex and transported to the vacuole via a prevacuolar endosome-like compartment. J. Cell Biol. *121*, 1245–1256.

Volland, C., Urban-Grimal, D., Géraud, G., and Haguenauer-Tsapis, R. (1994). Endocytosis and degradation of the yeast uracil permease under adverse conditions. J. Biol. Chem. *269*, 9833–9841.

Wilson, I.A., Niman, H.L., Houghten, A.R., Cherenson, M.L., Connolly, M.L., and Lerner, R.A. (1984). The structure of an antigenic determinant in a protein. Cell *37*, 767–778.

Wilson, K.L., and Herskowitz, I. (1984). Negative regulation of *STE6* gene expression by the α2 product of *Saccharomyces cerevisiae*. Mol. Cell. Biol. *4*, 2420–2427.

Wilson, K.L., and Herskowitz, I. (1986). Sequences upstream of the *STE6* gene required for its expression and regulation by the mating type locus in *Saccharomyces cerevisiae*. Proc. Natl. Acad. Sci. USA *83*, 2536–2540.

Woolford, C.A., Daniels, L.B., Park, F.J., Jones, E.W., Van Arsdell, J.N., and Innis, M.A. (1986). The *PEP4* gene encodes an aspartyl protease implicated in the posttranslational regulation of *Saccharomyces cerevisiae* vacuolar hydrolases. Mol. Cell. Biol. *6*, 2500–2510.